Construction of Porous Solids from Hydrogen-Bonded Metal Complexes of 1,3,5-Benzenetricarboxylic Acid

O. M. Yaghi,* Hailian Li, and T. L. Groy

Contribution from the Department of Chemistry and Biochemistry, Goldwater Center for Science and Engineering, Arizona State University, Tempe, Arizona 85287-1604

Received March 7, 1996. Revised Manuscript Received July 17, 1996[⊗]

Abstract: The reaction of M(II) acetate hydrate (M = Co, Ni, and Zn) with 1,3,5-benzenetricarboxylic (BTC) acid yields a material formulated as $M_3(BTC)_2{\cdot}12H_2O$. These compounds are isostructural as revealed by their XRPD patterns and a single crystal structure analysis performed on the cobalt containing solid [monoclinic, space group *C2*, $a = 17.482$ (6) Å, $b = 12.963$ (5) Å, $c = 6.559$ (2) Å, $\beta = 112.04°$, $V = 1377.8$ (8) Å, $Z = 4$]. This solid is composed of zigzag chains of tetra-aqua cobalt(II) benzenetricarboxylate that are hydrogen-bonded to yield a tightly held 3-D network. Upon liberating 11 water ligands per formula unit a porous solid results, $M_3(BTC)_2{\cdot}H_2O$, which was found to reversibly and repeatedly bind water without destruction of the framework. The proposed 1-D channels of the monohydrate have a pore diameter of 4 × 5 Å, which is typical of those observed in zeolites and molecular sieves. The successful inclusion of ammonia into the porous solid was demonstrated. Larger molecules and others without a reactive lone pair are disallowed from entering the channels.

Introduction

Controlling the assembly of molecules in the solid state is currently recognized as one of the most important issues in the synthesis of functional materials.[1] The successful pursuit of this challenge is expected to impact many technologies such as catalysis, nonlinear optics, microelectronics, sensors, and molecular recognition.[2] We and others have recently shown that intermolecular interactions such as metal-ligand coordination may be utilized in the directed assembly of a wide variety of 2-D and 3-D extended porous metal-organic networks[3] exhibiting unusual ion exchange,[3a,d] neutral guest exchange,[3e] and selective adsorptive[3c] behavior.

Presently, we are exploring the use of metal-ligand coordination along with intramolecular interactions toward the assembly of extended open-frameworks. Although hydrogen-bonding has been widely used to construct extended organic solids possessing both condensed and open structures,[4,5] strategies for their utility in assembling porous metal-organic frameworks remain, with the exception of few reports,[5c,6] largely unexplored. Given that hydrogen-bonding interactions are attractive, directional, and selective, it is not unreasonable to imagine many excellent opportunities for juxtaposing active groups within constructed frameworks such that they would impart certain desirable electronic, magnetic, or inclusion behavior on the material.

In the present study, we chose two simple building units, the organic ligand 1,3,5-benzenetricarboxylate (BTC), **a**, the metal aqua complex, **b**, to illustrate how by controlling the extent of

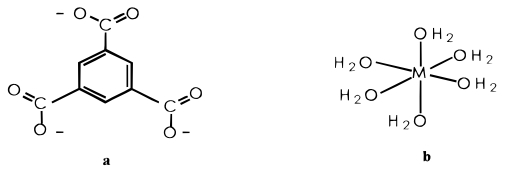

a **b**

hydration around the metal center a porous 3-D solid is produced. The essence of this synthetic approach is illustrated by a simple example representing a 2-D material shown in Figure 1. Here, metal-aqua centers are linked to BTC ligands by condensation polymerization to form an extended framework which has dangling water ligands that point toward the center of the voids. Each metal center is polymerized with BTC at two coordination sites leaving the remaining sites for associated water ligands. Since metal coordination to BTC is much stronger than it is to water, it is expected that water liberation by heating will be facilitated due to its weaker bonding to the

[⊗] Abstract published in *Advance ACS Abstracts,* September 1, 1996.

(1) (a) Amabilino, D. B.; Stoddart, J. F. *Chem. Rev.* **1995**, *95*, 2725−2828. (b) Herrmann, W. A.; Huber, N. W.; Runte, O. *Angew. Chem., Int. Ed. Engl.* **1995**, *34*, 2187−2206. (c) Schubert, U.; Hüsing, N.; Lorenz, A. *Chem. Mater.* **1995**, *7*, 2010−2027. (d) Stein, A.; Keller, S. W.; Mallouk, T. E. *Science* **1993**, *259*, 1558−1564. (e) Fagan, P. J.; Ward, M. D. *Sci. Am.* **1992**, *267*, 48−54. (f) Bein, T. *Supramolecular Architecture: Synthetic Control in Thin Films and Solids*; American Chemical Society: Washington, DC, 1992.

(2) (a) Miyasaka, H.; Matsumoto, N.; Okawa, H.; Re, N.; Gallo, E.; Floriani, C. *J. Am. Chem. Soc.* **1996**, *118*, 981−994. (b) Kobayashi, H.; Tomita, H.; Naito, T.; Kobayashi, A.; Sakai, F.; Watanabe, T.; Cassoux, P. *J. Am. Chem. Soc.* **1996**, *118*, 368−377. (c) Sato, O.; Iyoda, T.; Fujishima, A.; Hashimoto, K. *Science* **1996**, *271*, 49−51. (d) Day, P. *Science* **1993**, *261*, 431−432. (e) Bruce, D. W. *J. Chem. Soc., Dalton Trans.* **1993**, 2983−2989. (f) Simon, J.; Engel, M. K.; Soulié, C. *New J. Chem.* **1992**, *16*, 287−293. (g) Whitesides, G. M.; Mathias, J. P.; Seto, C. T. *Science* **1991**, *254*, 1312−1319. (h) Real, J. A.; Andrés, E.; Muñoz, M. C.; Julve, M.; Granier, T.; Bousseksou, A.; Varret, F. *Science* **1995**, *268*, 265−267. (i) Dagani, R. *Chem. Eng. News* **1991**, May 27, 24−30.

(3) (a) Yaghi, O. M.; Li, H. *J. Am. Chem. Soc.* **1996**, *118*, 295−296. (b) Robinson, F.; Zaworotko, M. J. *J. Chem. Soc., Chem. Commun.* **1995**, *23*, 2413−2414. (c) Yaghi, O. M.; Li, G.; Li, H. *Nature* **1995**, *378*, 703−706. (d) Yaghi, O. M.; Li, H. *J. Am. Chem. Soc.* **1995**, *117*, 10401−10402. (e) Gardner, G. B.; Venkataraman, D.; Moore, J. S.; Lee, S. *Nature* **1995**, *374*, 792−795. (f) Venkataraman, D.; Gardner, G. B.; Lee, S.; Moore, J. S. *J. Am. Chem. Soc.* **1995**, *117*, 11600−11601. (g) Subramanian, S.; Zaworotko, M. J. *Angew. Chem., Int. Ed. Engl.* **1995**, *34*, 2127−2129. (h) Fujita, M.; Kwon, Y. J.; Sasaki, O.; Yamaguchi, K.; Ogura, K. *J. Am. Chem. Soc.* **1995**, *117*, 7287−7288. (i) Lu, J.; Harrison, W. T. A.; Jacobson, A. J. *Angew. Chem., Int. Ed. Engl.* **1995**, *34*, 2557−2559. (j) Farrell, R. P.; Hambley, T. W.; Lay, P. A. **1995**, *34*, 757−758. (k) Batten, S. R.; Hoskins, B. F.; Robson, R. *J. Am. Chem. Soc.* **1995**, *117*, 5385−5386. (l) Schwarz, P.; Siebel, E.; Fischer, R. D.; Apperley, D. C.; Davies, N. A.; Harris, R. K. *Angew. Chem., Int. Ed. Engl.* **1995**, *34*, 1197−1199.

(4) (a) Russell, V. A.; Etter, M. C.; Ward, M. D. *J. Am. Chem. Soc.* **1994**, *116*, 1941−1952. (b) Garcia-Tellado, F.; Geib, S. J.; Goswami, S.; Hamilton, A. D. *J. Am. Chem. Soc.* **1991**, *113*, 9265−9269. (c) Etter, M. C. *Acc. Chem. Res.* **1990**, *23*, 120−126. (d) Seto, C. T.; Whitesides, G. M. *J. Am. Chem. Soc.* **1990**, *112*, 6409−6411.

(5) (a) Endo, K.; Sawaki, T.; Koyanagi, M.; Kobayashi, K.; Masuda, H.; Aoyama, Y. *J. Am. Chem. Soc.* **1995**, *117*, 8341−8352. (b) Venkataraman, D.; Lee, S.; Zhang, J.; Moore, J. S. *Nature* **1994**, *371*, 591−593. (c) Wang, X.; Simard, M.; Wuest, J. D. *J. Am. Chem. Soc.* **1994**, *116*, 12119−12120. (d) Ermer, O.; Lindenberg, L. *Helv. Chim. Acta* **1991**, *74*, 825−877.

(6) Copp, S. B.; Subramanian, S.; Zaworotko, M. J. *Angew. Chem., Int. Ed. Engl.* **1993**, *32*, 706−709.

S0002-7863(96)00746-9 CCC: $12.00

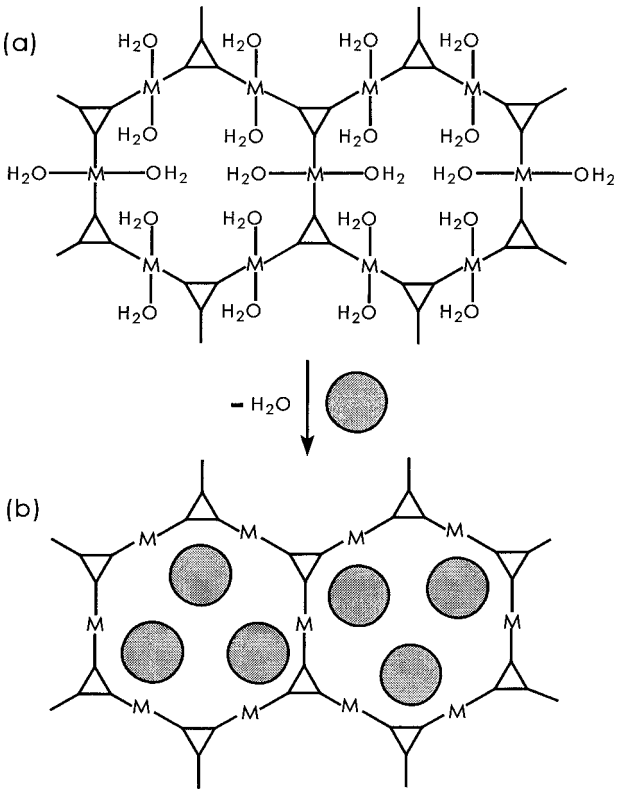

Figure 1. A schematic representation of (a) a 2-D assembly of metal (M) aqua complexes and trigonal trifunctional building units (triangles) to form extended layers having no voids and (b) a porous structure with molecular guests (large filled spheres) occupying the void space resulting from the liberation of water ligands from those layers.

framework. This yields an open-framework having voids that are decorated by coordinately unsaturated metal centers, which consequently are capable of serving as binding sites to other inclusions. In such an open framework, the selective inclusion of incoming molecular guests is dependent not only on their size and shape but also on their electronic affinity for the metal center. Thus, the process of separating molecules of similar shape and size becomes viable.

By manipulating the intermolecular (M−BTC and M−OH_2 coordination) and the intramolecular (COO−−H_2O hydrogen bonding) interactions, it is possible to organize 1-D polymeric M−BTC chains into porous solids. This is only possible if the interactions within the backbone of the assembled supramolecular structure are stronger than those existing elsewhere in the solid, since it is the latter interactions that must be overcome to yield a porous network. Using this principle, a porous network should be produced upon replacing the metal centers (lying along the same horizontal line in Figure 1a), linking what can be viewed as two zigzag chains, with ligands capable of $\pi-\pi$ or hydrogen-bonding interactions that are strong enough to hold the chains together in the absence of inclusions. These structural features and events are exemplified by the synthesis, structure, and inclusion properties of the hydrated 1-D hydrogen-bonded solid, $M_3(BTC)_2{\cdot}12H_2O$ (M = Co, Ni, and Zn) described herein.

Experimental Section

Materials and Methods. Cobalt(II) acetate tetrahydrate was purchased from J. T. Baker Chemical Company. All other materials were purchased from Aldrich Chemical Company and used as received, without further purification. Elemental microanalysis of products were performed on crystalline samples by the School of Chemical Sciences Microanalytical Laboratory at the University of Illinois-Urbana and at Arizona State University Materials Facility using a Perkin-Elmer 2400 CHNS analyzer. Thermogravimetric analysis was performed under He and at a scan rate of 0.5 °C/min using a Setaram TG92 system.

Infrared spectra were measured from KBr pellets using a Nicolet FT-IR Impact 400 system. Solid-state ^{13}C NMR spectra were recorded on a Varian Unity Plus-400 spectrometer by using a 5 mm cross-polarization magic angle spinning (CP MAS) probe. Chemical shifts were referenced externally to tetramethylsilane (δ 0 ppm) using solid hexamethylbenzene (δ 17.3 ppm) as a secondary reference. X-ray powder diffraction (XRPD) data was recorded on a Rigaku D/Max-IIB diffractometer at 50 kV, 30 mA for Cu Kα, (λ = 1.5406 Å) with a scan speed of 2°/min and a step size of 0.02° in 2θ. The calculated XRPD patterns were produced using the SHELXTL-XPOW program with the single crystal data.

Preparation of Compounds. The synthetic methods used to obtain microcrystalline and large single crystal samples of the compounds, including their initial characterization are described here. Unless otherwise indicated all reactions and purification steps were performed under aerobic conditions.

$M_3(BTC)_2{\cdot}12H_2O$ (M = Co, Ni, and Zn). Identical synthetic procedures were used to prepare the three compounds, that of the cobalt compound is described here in detail. An aqueous mixture (15 mL) of cobalt(II) acetate tetrahydrate (0.41 g, 1.65 mmol) and the acid form of BTC ($BTCH_3$) (0.20 g, 0.95 mmol) was placed in a stainless steel vessel, which was sealed and placed in a programmable furnace. The mixture was heated to 140 °C at 5 °C/min and held at that temperature for 24 h, then cooled at 0.1 °C/min to 120 °C and held for 5 h, followed by further cooling at the same rate to 100 °C, and held for another 5 h before finally cooling to room temperature. The resulting large rod-like red crystals were filtered, washed with deionized water (3 × 10 mL) and ethanol (3 × 10 mL), and then air-dried to give 0.33 g (86%) of $Co_3(BTC)_2{\cdot}12H_2O$. Crystalline samples of this solid are stable and insoluble in water, ethanol, acetonitrile, chloroform, tetrahydrofuran, acetone, and *N*,*N*-dimethylformamide. However, this compound shows limited stability in methanol. Anal. Calcd for $C_{18}H_{30}O_{24}Co_3$ = $Co_3(BTC)_2{\cdot}12H_2O$: C, 26.78; H, 3.75; Co, 21.90. Found: C, 26.72; H, 3.64; Co, 21.58. FT-IR (KBr, 3500−400 cm^{-1}): 3467 (vs, broad), 3124 (vs, broad), 2269 (w), 1848 (w), 1700 (sh), 1624 (vs), 1565 (sh), 1532 (vs), 1479 (s), 1440 (vs), 1374 (vs), 1216 (w), 1117 (w), 1038 (sh), 986 (w), 933 (w), 907 (w), 821 (m), 769 (s), 723 (vs), 663 (sh), 571 (s), 538 (m), 466 (m), 446 (m), 426 (m).

Thermal gravimetric analysis performed under a flow of helium gas on a 29.38 mg sample of this material shows onset of weight loss at 110 °C. Water removal continues up to 345 °C to give a total weight loss of 7.85 mg (26.7%), which is the equivalent to losing 12 H_2O molecules per formula unit (calculated value = 26.8%). The complete decomposition of the sample is achieved at 500 °C.

The nickel(II) analogue was prepared using an identical procedure, where light green microcrystals are obtained. Single crystals of this solid were grown and selected from a 10 mL mixture of nickel(II) acetate tetrahydrate (0.35 g, 1.41 mmol) and $BTCH_3$ (0.10 g, 0.48 mmol) that was heated to 170 °C for 12 h before cooling to room temperature. Anal. Calcd for $C_{18}H_{30}O_{24}Ni_3$ = $Ni_3(BTC)_2{\cdot}12H_2O$: C, 26.80; H, 3.75; Ni, 21.84. Found: C, 26.74; H, 3.63; Ni, 21.72. FT-IR (KBr, 3500−400 cm^{-1}): 3454 (vs, broad), 3125 (s, broad), 2295 (w), 1848 (w), 1690 (sh), 1614 (vs), 1564 (sh), 1523 (vs), 1479 (s), 1436 (vs), 1377 (vs), 1216 (w), 1111 (w), 1044 (w), 994 (w), 929 (w), 915 (w), 821 (m), 760 (s), 728 (vs), 663 (sh), 572 (m), 532 (m), 464 (m), 426 (w).

The zinc(II) analogue was prepared as needle-like colorless single crystals using an identical procedure to that described for the cobalt compound. Anal. Calcd for $C_{18}H_{30}O_{24}Zn_3$ = $Zn_3(BTC)_2{\cdot}12H_2O$: C, 26.16; H, 3.66; Zn, 23.73. Found: C, 26.35; H, 3.52; Zn, 22.96. FT-IR (KBr, 3500−400 cm^{-1}): 3447 (vs, broad), 3125 (s, broad), 2295 (w), 1624 (vs), 1532 (vs), 1479 (m), 1440 (vs), 1381 (vs), 1117 (w), 992 (w), 933 (w), 814 (m), 769 (s), 729 (vs), 571 (m), 532 (w), 459 (w). ^{13}C CP MAS NMR: δ 125.8 and 133.3 (s, $\boldsymbol{C}_6H_3(COO)_3$), 172.4 and 178.4 (s, $C_6H_3(\boldsymbol{C}OO)_3$).

The phase purity of the bulk products for the compounds reported here were confirmed by comparison of the observed and calculated XRPD patterns. Typical agreement between calculated and experimental patterns is presented in Figure 2.

$Co_3(BTC)_2{\cdot}xH_2O$ (x = 6, 4, 2, and 1). Red crystals in the size range (0.1−0.3 mm) of $Co_3(BTC)_2{\cdot}12H_2O$ (0.30 g) were heated at 0.080

Table 1. Calculated and Found (*Italics*) Percent Composition Values for the Hydrated and Partially Dehydrated Solids

compd	C	H	M
$Co_3(BTC)_2 \cdot 12H_2O$	26.78	3.75	21.90
	26.72	*3.64*	*21.58*
$Co_3(BTC)_2 \cdot 6H_2O$	30.92	2.59	
	30.90	*2.25*	
$Co_3(BTC)_2 \cdot 4H_2O$	32.60	2.13	
	32.42	*2.05*	
$Co_3(BTC)_2 \cdot 2H_2O$	34.47	1.61	
	34.32	*1.49*	
$Co_3(BTC)_2 \cdot H_2O$	35.44	1.32	
	35.33	*1.38*	
$Ni_3(BTC)_2 \cdot 12H_2O$	26.80	3.75	21.84
	26.74	*3.63*	*21.72*
$Ni_3(BTC)_2 \cdot H_2O$	35.54	1.36	
	35.23	*1.43*	
$Zn_3(BTC)_2 \cdot 12H_2O$	26.16	3.66	23.73
	26.35	*3.52*	*22.96*
$Zn_3(BTC)_2 \cdot H_2O$	34.40	1.28	
	34.54	*1.27*	

Table 2. Calculated and Found (*Italics*) Percent Composition Values for the Inclusion of H_2O and NH_3 in $M_3(BTC)_2 \cdot H_2O$

compd	C	H	N	M
$Co_3(BTC)_2 \cdot 12H_2O$	26.78	3.75		21.90
	26.52	*3.70*		*21.10*
$Co_3(BTC)_2 \cdot 4H_2O \cdot 15NH_3$	23.54	6.47	22.87	
	23.28	*6.44*	*22.51*	
$Ni_3(BTC)_2 \cdot 12H_2O$	26.80	3.75		
	25.98	*3.86*		
$Ni_3(BTC)_2 \cdot 3H_2O \cdot 17NH_3$	23.15	6.80	25.51	
	23.33	*6.72*	*25.73*	
$Zn_3(BTC)_2 \cdot 12H_2O$	26.16	3.66		23.73
	26.03	*3.57*		*23.93*
$Zn_3(BTC)_2 \cdot 2H_2O \cdot 10NH_3$	26.47	4.94	17.15	
	26.98	*4.39*	*17.35*	

Torr to 80 °C for 1.5 h, at 0.080 Torr to 80 °C for 3h, at 0.080 Torr to 90 °C for 8 h, and at atmospheric pressure to 250 °C for 4 h to yield, respectively, the blue solids formulated as $Co_3(BTC)_2 \cdot 6H_2O$, $Co_3(BTC)_2 \cdot 4H_2O$, $Co_3(BTC)_2 \cdot 2H_2O$, and $Co_3(BTC)_2 \cdot H_2O$. Elemental microanalyses of these products are included in Table 1. FT-IR for $Co_3(BTC)_2 \cdot H_2O$ (KBr, 3500−400 cm^{-1}): 3441 (s, broad), 3078 (m, broad), 2295 (w), 1631 (vs), 1545 (vs), 1453 (s), 1374 (vs), 1200 (sh), 1124 (w), 933 (w), 814 (w), 762 (s), 723 (s), 571 (m), 472 (w), 453 (w). The nickel monohydrate was prepared using analogous procedure (see Table 1).

$Zn_3(BTC)_2 \cdot H_2O$. Colorless crystals in the size range (0.1−0.3 mm) of $Zn_3(BTC)_2 \cdot 12H_2O$ (0.30 g) were heated at 0.080 Torr to 150 °C for 5 h to give $Zn_3(BTC)_2 \cdot H_2O$. Elemental microanalysis of this product is presented in Table 1. FT-IR for $Zn_3(BTC)_2 \cdot H_2O$ (KBr, 3500−400 cm^{-1}): 3441 (s, broad), 3085 (m, broad), 1631 (vs), 1552 (vs), 1446 (s), 1387 (vs), 1200 (sh), 1124 (w), 940 (w), 769 (s), 729 (s), 577 (m), 472 (w).

Inclusion Studies. Typically, freshly prepared monohydrate solids of $M_3(BTC)_2 \cdot H_2O$ (M = Co, Ni, or Zn) were either exposed to the gaseous form of the incoming guest for the duration of 16 h or soaked in the neat solution of the guest for 5 min. Then isolated and, in the cases of liquid guest inclusion, washed several times with ethanol and diethyl ether followed by air drying for at least 3 h. Ammonia gas was produced by the addition of sodium hydroxide solid to a 30% aqueous solution of ammonium hydroxide. Successful absorption and desorption of only H_2O and NH_3 was achieved by these solids giving no evidence for the inclusion of other molecules such as CO, CO_2, CS_2, H_2S, CH_3CN, and NC_5H_5. A summary of the formulated inclusion products is presented in Table 2.

X-ray Data Collection and Reduction. Crystallographic details of the nickel and zinc compounds will not be presented since crystalline samples of these compounds were found to have identical cell parameters and PXRD to that of $Co_3(BTC)_2 \cdot 12H_2O$. A complete single crystal analysis study was undertaken on this compound, and the experimental details for the structure determination are given in Table 3. A pale red single crystal (0.50 × 0.17 × 0.17 mm) was separated from the reaction product and attached to a glass fiber using epoxy. Data were collected on a Siemens R3m/V autodiffractometer using graphite-monochromated Mo Kα radiation and full 1.60° wide ω scans to a maximum of $\theta = 25.08°$, giving 2628 unique reflections. Lattice parameters were obtained from least-squares analyses of 25 computer-centered reflections with $15 \leq 2\theta \leq 30$. The raw intensity data was converted to structure factor amplitudes and their estimated standard deviations by correction for scan speed, background, and Lorentz and polarization effects using XDISK facility within the SHELXTL PLUS package. The data were corrected for absorption using ψ-scan data from six reflections covering the range of data collection with resultant maximum and minimum transmission values of 0.725 and 0.388. The compound crystallized in the monclinic system and statistics identified the space group as *C*2 which was consistent with all stages of the subsequent structure determination and refinement.

Structure Solution and Refinement. The asymmetric unit consists of two cobalt(II) centers, one of which (Co1) is on a 2b site (0.5, 0.8448, 0.5), one full BTC, and six water molecules as ligands on the cobalt centers, which produces the stoichiometry of $Co_3(BTC)_2 \cdot 12H_2O$. The initial structure solution was performed using direct methods in SHELXTL PC rel. 5.03 (Siemens Analytical X-ray Instruments, 1994). The approximate positions of all but two of the non-hydrogen atoms were easily discernable. Subsequent full least-squares refinement on weighted F^2 using the same package and interpretation of Fourier difference maps revealed the two remaining non-hydrogen atoms. Refinement of the Flack x parameter[7] indicated that the structure actually contains 58.5% of the racemate vide infra and 41.5% of the corresponding racemic twin. In the final stages, hydrogens were placed as riding atoms on their corresponding bonding sites. Final R indices for the observed data are shown in Table 3. A goodness-of-fit of 1.088 was achieved. The final largest difference peak and hole were 0.609 and −0.299 $e^-/Å^3$. Convergence of the refinement occurred with the largest and mean Δ/σ being −0.004 and 0.000, respectively.

Results and Discussion

Synthesis and Structure of $M_3(BTC)_2 \cdot 12H_2O$ (M = Co, Ni and Zn). The hydrothermal reaction of metal(II) acetate hydrate with 1,3,5-benzenetricarboxylic acid ($BTCH_3$) in approximately 3:2 mole ratio at 140 °C yields red (Co), green (Ni), and colorless (Zn) crystals, which had elemental analysis (Table 1) consistent with the formula $M_3(BTC)_2 \cdot 12H_2O$. These compounds show identical infrared spectra with the absorption bands of the asymmetric and symmetric vibration of BTC respectively appearing at 1564−1532 and 1479−1374 cm^{-1}. The broad bands at 3467−3125 cm^{-1} and the sharp band at 1624 cm^{-1} are indicative of the presence of water in the metal coordination sphere. The absence of absorption bands at 1730−1690 cm^{-1} where the -COOH is expected to appear, is indicative of the deprotonation of $BTCH_3$ upon its reaction with metal ions.[8]

These compounds are isostructural as they show identical XRPD patterns, which agree closely with those calculated using the single crystal structure data obtained for the cobalt compound (compare Figure 2a,b). A single-crystal structure analysis performed on the $Co_3(BTC)_2 \cdot 12H_2O$ compound shows that the structure is composed of zigzag chains constructed from two symmetry-inequivalent tetra-aqua cobalt(II) units and BTC ligands as shown in Figure 3. Crystal data, atomic coordinates, and selected bond lengths and angles are given in Tables 3−5, respectively. The bond length and angle values show no deviation from those observed for other metal carboxylate complexes.[9]

Two of the carboxylate units (O2, O3 and O2A, O3A) of BTC bind in a unidentate fashion to the axial positions of two

(7) (a) Flack, H. D. *Acta Crystallogr.* **1983**, *A39*, 876−881; (b) Bernardinelli, G.; Flack, H. D. *Acta Crystallogr.* **1985**, *A41*, 500−511.

(8) (a) Brzyska, W.; Sadowski, P. *Pol. J. Chem.* **1987**, 61, 273−279. (b) Brzyska, W.; Wolodkiewicz, W. *Pol. J. Chem.* **1986**, 60, 697−702. (c) Wieghardt, K. *JCS Dalton* **1973**, 2548−2552. (d) Bellamy, L. J. *The Infrared Spectra of Complex Molecules*; Wiley: New York, 1958.

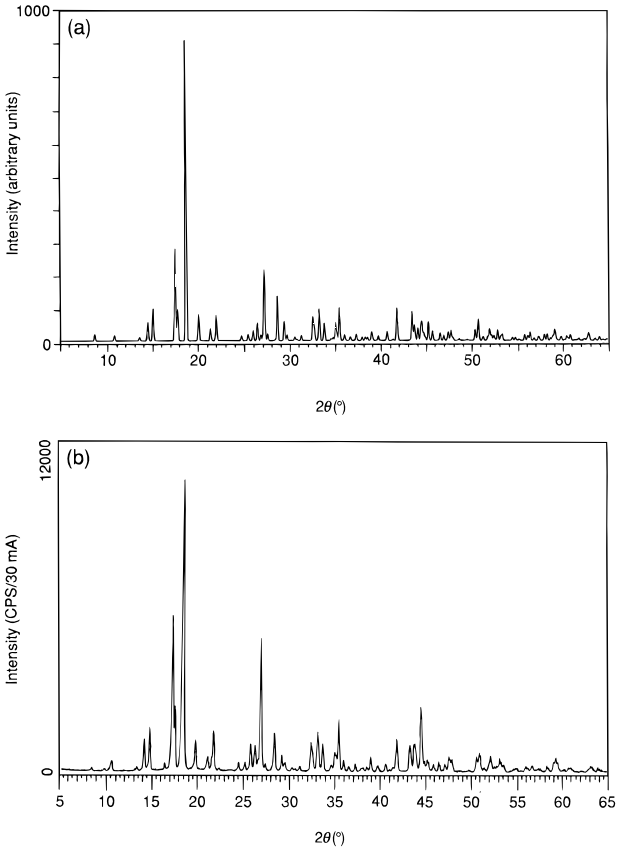

Figure 2. Calculated (a) and observed (b) X-ray powder diffractions patterns for the starting crystalline isostructural solids, $M_3(BTC)_2 \cdot 12H_2O$ (M = Co, Ni, and Zn).

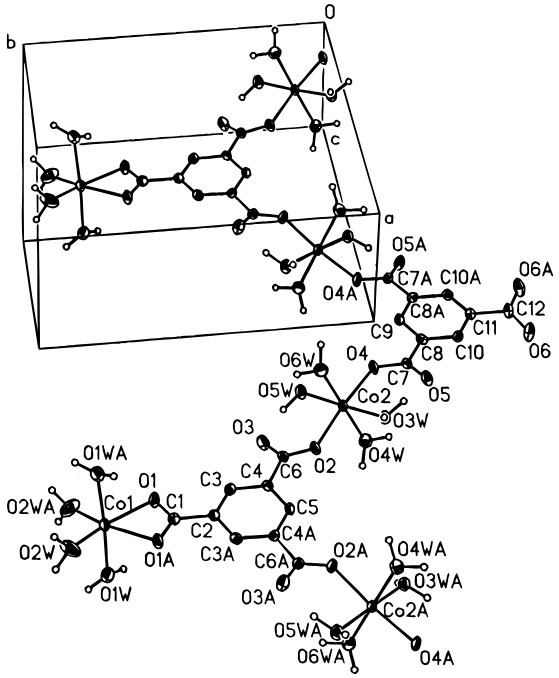

Figure 3. The Co-BTC chain, including the asymmetric unit, present as the building block in crystalline $Co_3(BTC)_2 \cdot 12H_2O$. The non-hydrogen atoms are represented by thermal ellipsoids drawn to encompass 50% of their electron density. Atoms labeled with additional letter A are symmetry equivalent to those atoms without such designation. The hydrogen atoms on BTC are not shown, but those of water are drawn using an arbitrary sphere size for clarity.

nearly perfect octahedral and symmetry-equivalent cobalt centers (Co2 and Co2A), while the third carboxylate (O1, O1A) binds in a bidentate fashion to the equatorial positions of a third, but

Table 3. Crystallographic Data for $Co_3(BTC)_2 \cdot 12H_2O$

formula	$C_{18}H_{30}O_{24}Co_3$
M	807.22
crystal system	monoclinic
space group	*C*2
a, Å	17.482 (6)
b, Å	12.963 (5)
c, Å	6.559 (2)
β, °	112.04
Z	4
V, Å^3	1377.8 (8)
d_{calc}, g/cm^3	1.946
μ, mm^{-1}	1.892
$R(R_w)$	0.0226 (0.0572)
weighting scheme, w^{-1}	$\sigma^2(F_o^2) + (0.0371P)^2 + 0.6338P$, $P = (F_o^2 + 2F_c^2)/3$

Table 4. Atomic Coordinates [$\times 10^4$] and Equivalent Isotropic Displacement Parameters [Å$^2 \times 10^3$] for $Co_3(BTC)_2 \cdot 12H_2O$

atom	*x*	*y*	*z*	*U*(eq)
Co(1)	5000	8448(1)	5000	20(1)
Co(2)	7582(1)	1324(1)	7846(1)	17(1)
O(1W)	5572(1)	8501(2)	8500(4)	33(1)
O(2W)	4167(2)	9410(2)	5385(4)	49(1)
O(3W)	6780(1)	264(2)	8423(4)	22(1)
O(4W)	7346(1)	660(2)	4693(3)	28(1)
O(5W)	8404(1)	2430(2)	7475(4)	25(1)
O(6W)	7785(1)	1956(2)	11015(4)	32(1)
O(1)	5649(1)	7019(2)	5213(4)	24(1)
O(2)	6575(1)	2274(2)	6468(4)	22(1)
O(3)	7158(1)	3720(2)	5917(4)	28(1)
O(4)	8532(1)	272(1)	9023(4)	24(1)
O(5)	7857(1)	−1164(2)	9170(4)	26(1)
O(6)	9312(1)	−4545(2)	9349(4)	32(1)
C(1)	5000	6514(3)	5000	20(1)
C(2)	5000	5381(3)	5000	17(1)
C(3)	5729(2)	4841(2)	5396(4)	18(1)
C(4)	5738(2)	3770(2)	5426(4)	16(1)
C(5)	5000	3231(3)	5000	16(1)
C(6)	6553(2)	3212(2)	5977(4)	16(1)
C(7)	8489(2)	−690(2)	9226(4)	17(1)
C(8)	9266(2)	−1295(2)	9603(4)	17(1)
C(9)	10000	−758(3)	10000	17(1)
C(10)	9266(2)	−2368(2)	9599(4)	18(1)
C(11)	10000	−2911(3)	10000	16(1)
C(12)	10000	−4071(3)	10000	21(1)

Table 5. Selected Bond Lengths and Angles for $Co_3(BTC)_2 \cdot 12H_2O$

distances	[Å]	angles	[deg]
Co(1)−O(2W)	2.004(2)	O(2W)−Co(1)−O(2WA)	103.1(2)
Co(1)−O(1W)	2.133(2)	O(2WA)−Co(1)−O(1WA)	85.1(1)
Co(1)−O(1)	2.151(2)	O(2WA)−Co(1)−O(2W)	92.7(1)
Co(2)−O(4)	2.062(2)	O(2W)−Co(1)−O(1A)	98.8(1)
Co(2)−O(5W)	2.107(2)	O(2W)−Co(1)−O(1)	156.8(1)
Co(2)−O(6W)	2.136(2)	O(1A)−Co(1)−O(1)	60.9(1)
		O(2)−Co(2)−O(4)	174.8(1)
		O(4)−Co(2)−O(3W)	89.9(1)
		O(4)−Co(2)−O(5W)	90.3(1)

symmetry-inequivalent and distorted, octahedral cobalt center (Co1). Water ligands O3W and O5W on Co2 are engaged in hydrogen bonding, respectively, to carboxylate oxygens O5 and O3 of an adjacent BTC within the chain, while O2W and O2WA on Co1 are hydrogen-bonded to O3W and O5W of an adjacent chain to form hydrogen-bonded layers. These layers are held together by similar but more numerous hydrogen bonding interactions involving every remaining water and carboxylate unit in the structure to yield a tightly held 3-D solid having a

(9) (a) Pech, R.; Pickardt, J. *Acta Crystallogr.* **1988**, *C44*, 992−994. (b) Chaudhuri, P.; Oder, K.; Wieghardt, K.; Gehring, S.; Haase, W.; Nuber, B.; Weiss, J. *J. Am. Chem. Soc.* **1988**, *110*, 3657−3658. (c) Poleti, D.; Stojakovic; Prelesnik, B. V.; Herak, R. M. *Acta Crystallogr.* **1988**, *C44*, 242−245.

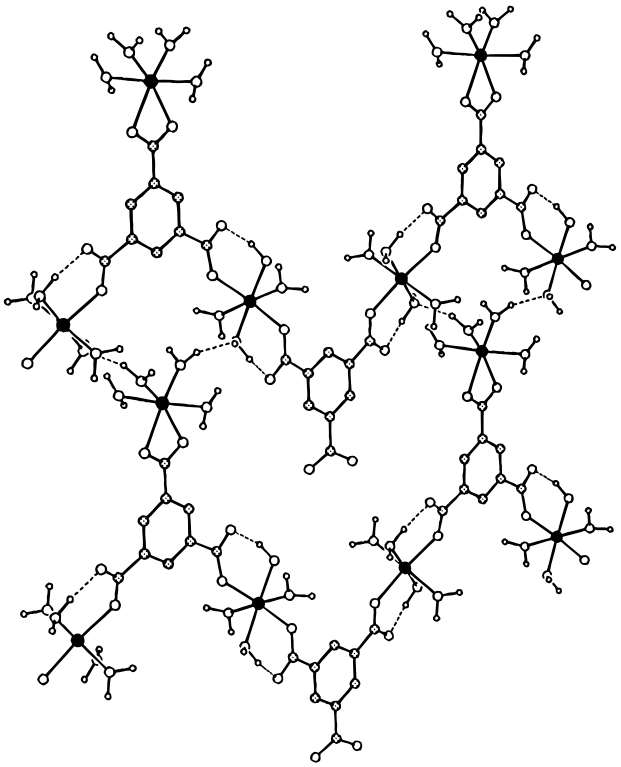

Figure 4. A view of two adjacent Co-BTC chains (Co, dark; C; shaded; O, Open; H, small) showing the zigzag topology of the chains, propagating along the *a*-axis, and their association by hydrogen bonding (dotted lines).

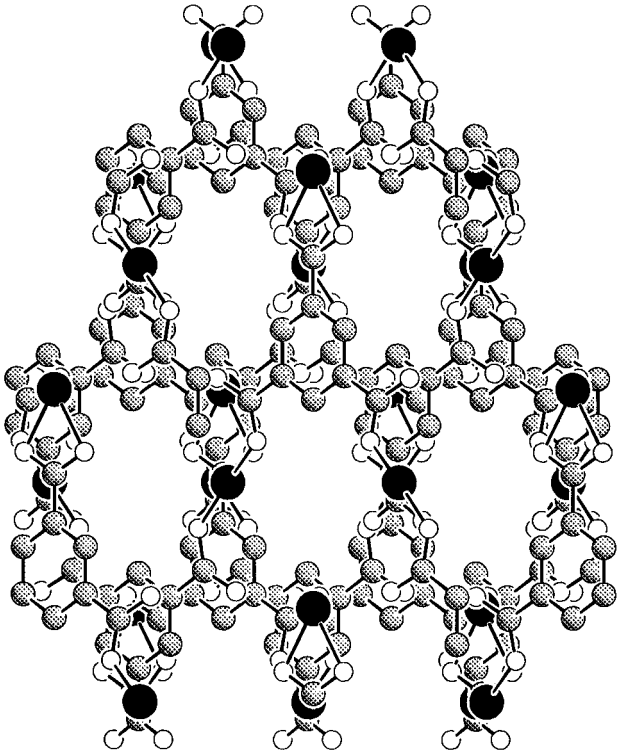

Figure 5. A projection approximately perpendicular to the crystallographic *c*-axis showing the open-channel system resulting by liberating the aqua ligands in crystalline $Co_3(BTC)_2 \cdot 12H_2O$. Coordinately unsaturated Co(II) centers (dark spheres) decorate the channels and are believed to be the site of guest reversible binding. The hydrogen atoms on BTC are omitted for clarity.

total of 56 hydrogen bonding interactions per formula unit (12/cobalt tetra-aqua center and 10/BTC), which range from what is considered strong, 2.554(4) Å, to those considered weak, 3.120(5) Å, hydrogen bonds.[10]

Dehydration and Absorption Studies. It is instructive to view two adjacent Co-BTC chains according to Figure 4, where their zigzag shape leads to the positioning of three $Co(H_2O)_4$ units in the same vicinity. The noted clustering of metal-aqua units point to the possibility of removing the water ligands to create voids, which when stacked in the crystal should form channels. A thermal analysis study on this solid showed that these water ligands are easily removed in that water begins to dissociate and leave the structure at 110 °C and continues until the sample is completely dehydrated at 345 °C. In fact, if the water ligands are not included in the overall representation of the structure, an extended 1-D channel system with an elliptically-shaped pore of nearly 4×5 Å[11] diameter can be discerned as shown in Figure 5. Given that the size and shape of the pores in this structure are similar to those present in zeolites and molecular sieves such as ZSM-5, ZSM-11, and Zeolite-A,[12] which are known to exhibit diverse inclusion chemistry of small molecules such as O_2, N_2, CO, H_2O, and NH_3, it was not unreasonable to pursue the inclusion of these molecules into the dehydrated compound. Indeed attempts in this direction yielded a porous material capable of reversible inclusion of water and ammonia.

A series of experiments performed using a crystalline sample of $Co_3(BTC)_2 \cdot 12H_2O$ showed a sequential loss of 6, 8, 10, and 11 water molecules per formula unit upon heating the red solid to form a dark blue monohydrate solid, which was formulated as $Co_3(BTC)_2 \cdot H_2O$. The nickel and zinc monohydrate analogues have also been prepared in the same way and formulated by elemental microanalysis (shown in Table 1). The XRPD patterns for the monohydrates show very broad peaks indicating poor crystallinity and possible deformation of the framework as a result of liberating water. However, structural order and crystallinity are reestablished upon exposing the monohydrates to water as confirmed by the XRPD of the rehydrated solids and their elemental analysis. For the zinc compound, this transformation was achieved without leaving an imprint on the framework, as no broadening of the peaks and no change in their intensity was observed (Figure 6) compared to those of the fully hydrated starting material (Figure 2). ^{13}C CPMAS study on the rehydrated material show the same number of peaks and identical chemical shifts to those observed for the starting material. However, for the Co and Ni compounds the peak width and intensity of the XRPD pattern are slightly altered indicating that some deformation to the framework has occurred upon rehydration. The formulation for the rehydrated products are shown in Table 2, where the expected values for the regenerated starting materials, $M_3(BTC)_2 \cdot 12H_2O$, are within close agreement to those calculated values.

The reactive nature of the Co and Ni frameworks was further revealed when their monohydrates were exposed to $NH_{3(g)}$ at room temperature. Elemental microanalysis on the products gave a nitrogen value higher than that expected for the inclusion of 11 ammonia molecules per $(Co, Ni)_3(BTC)_2 \cdot H_2O$ unit (Table 2), which seems to indicate either partial dissociation of the

(10) (a) Jeffrey, G. A.; Saenger, W. *Hydrogen Bonding in Biological Structures*; Springer: Berlin, 1991. (b) Lehn, J. M. *Angew. Chem., Int. Ed. Engl.* **1990**, *29*, 1304. (c) Zerkowski, J. A.; Seto, C. T.; Wierda, D. A.; Whitesides, G. M. *J. Am. Chem. Soc.* **1990**, *112*, 9025. (d) Desiraju, G. R. *Crystal Engineering: The Design of Organic Solids*; Elsevier: New York, 1989, pp 115−173. (e) Emsley, J. *Chem. Soc. Rev.* **1980**, *91*. (f) Semmington, D. *Acta Chem. Scand., Ser. A* **1976**, *30*, 808. (g) Wang, Y.; Stucky, G. D. *J. Chem. Soc., Perkin Trans.* **1974**, *2*, 925.

(11) Cross-section value was calculated using van der Waals radii for carbon (1.70 Å) and oxygen (1.40 Å).

(12) (a) Davis, M. E.; Lobo, R. F. *Chem. Mater.* **1992**, *4*, 746−768. (b) Meier, W. M.; Olson, D. H. *Atlas of Zeolite Structure Types*; Butterworth-Heinemann: London, 1992. (c) Breck, D. W. *Zeolite Molecular Sieves*; Wiley: New York, 1984.

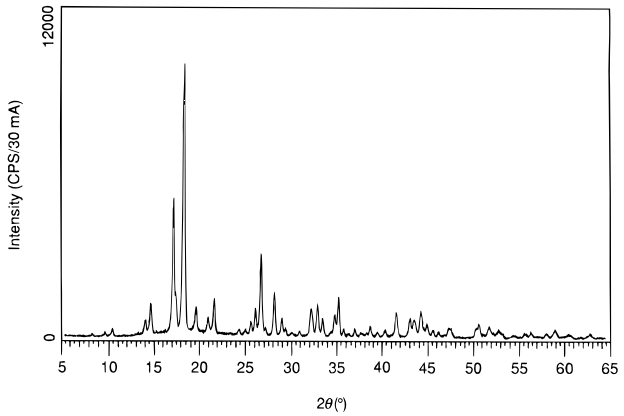

Figure 6. XRPD pattern of rehydrated $Zn_3(BTC)_2 \cdot H_2O$ (compare to Figure 2).

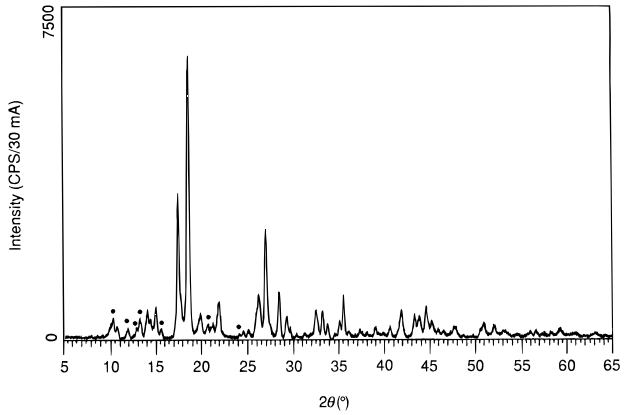

Figure 7. XRPD pattern of $Zn_3(BTC)_2 \cdot 12H_2O$ after the cycle of dehydration, ammonia inclusion, and removal, followed by water absorption.

metal from BTC within the framework or intercalation of ammonia between two BTC units which are part of different but adjacent chains. Also, their XRPD patterns show very broad peaks indicating poor crystallinity of the sample. However, deformation of the porous framework was not observed for the Zn analogue but instead the dehydrated sample absorbs the expected amount of inclusions per open coordination site on the Zn (ten ammonia molecules plus an additional water) to give a material formulated as $Zn_3(BTC)_2 \cdot 2H_2O \cdot 10NH_3$ (Table 2). We found that this solid may be converted back to $Zn_3(BTC)_2 \cdot 12H_2O$ by desorption of ammonia at 250 °C and 0.080 pressure for 5 h, followed by the addition of water at room temperature as shown in Figure 7. Here, the XRPD pattern of the fully hydrated material is obtained in addition to few unidentified peaks (marked with dark filled circles), possibly indicating the presence of a new phase, which was difficult to identify due to its poor yield.

Structural Integrity of $Zn_3(BTC)_2 \cdot H_2O$. It is worth noting that the presence of the last water ligand in the $M_3(BTC)_2 \cdot H_2O$ framework is a least necessary prerequisite for the observed inclusion behavior, which might be due to its unique ability to maintain the structural arrangement of the porous framework using hydrogen bonds. Its structure could not be confirmed unequivically due to its poor crystallinity; however, several indications point to the fact that it is maintained in the case of zinc during the inclusion process. First, its infrared spectrum shows that the prominent bands are coincident with those of the starting material. The absence of -COOH absorption bands ($1730-1690$ cm^{-1}) shows that BTC is bound at least in a monodentate fashion to the metal center. Second, its elemental microanalysis shows close agreement with the proposed formula indicating no ligand loss has occurred. Also, no evidence of molecular species in the supernatent during the inclusion process was detected. Third, especially in the zinc compound, the reversibility of inclusion into the monohydrate and its complete conversion to the starting material indicate the absence of any competing formation pathways. Fourth and most significant, the inclusion of water is facile process that is completed as soon as the solid is immersed into the liquid. This excludes the possibility of the material dissolving during inclusion and then recrystallizating as the fully hydrated material.

Attempts to include other small molecules into the porous solid were unsuccessful, in that we found no evidence for the inclusion of CO, CO_2, H_2S, CS_2, CH_3CN, and NC_5H_5. It appears that $M_3(BTC)_2 \cdot H_2O$ has high affinity toward small guests with reactive lone electron pair(s) (H_2O and NH_3), and little or no affinity toward others with relatively unreactive lone pair(s) (CO and CO_2). It was observed that H_2S reacts with the solid to produce a condensed phase. Larger molecules (CS_2, CH_3CN, and NC_5H_5) are not allowed into the channels due to steric constraints. The differences in inclusion behavior between this framework and zeolites are due to the intrinsic coordination chemistry governing the interaction of the metal center with the incoming molecules.

Summary

The following are the principal results and conclusions from this investigation.

(1) Dehydration of the extended hydrogen-bonded network of $M_3(BTC)_2 \cdot 12H_2O$ (M = Co, Ni and Zn) yields the monohydrate, $M_3(BTC)_2 \cdot H_2O$, which has a proposed porous structure with 1-D extended channels and a pore size comparable to those found in zeolites and molecular sieves. This identifies a strategy that can be extended to other 0-D, 1-D, and 2-D hydrogen-bonded structures which may initially have condensed structure with no voids, but can be made porous as a consequence of removing those loosely bound ligands.

(2) Inclusion of water and ammonia has been demonstrated; however, no evidence was found for the inclusion of other molecules of larger size and or having poor affinity to the metal center. The zinc compound shows that the desorption−reabsorption cycle of water occurs without affecting the porous framework as the XRPD of the final material is exactly identical to that of the solid present before initiation of the cycle, which was confirmed by their identical peak width, position and intensity. The diverse but specific coordination chemistry of the metal center and its positioning within the framework allows for combining shape and size selective inclusion with site directed and electronically driven inclusion.

These findings provide a clear connection between the well-established and vast ligand substitution chemistry of soluble metal complexes and its application along with hydrogen-bonding in the construction of open-frameworks having diverse architecture and function.

Acknowledgment. The financial support of this work by the National Science Foundation (CHE-9522303) and the technical assistance of Mr. Charles Davis and Dr. Ronald Nieman in collecting the solid state NMR data are gratefully acknowledged.

Supporting Information Available: Crystallographic data for $Co_3(BTC)_2 \cdot 12H_2O$ including crystal structure analysis reports and tables of positional parameters, thermal parameters, and interatomic distances and angles (8 pages). See any current masthead page for ordering and Internet access instructions.

JA960746Q